

RF ELECTRON SOURCE DESIGN MODELLING FOR OPTIMIZATION OF INITIAL e^- BEAM PARAMETERS FOR LCS γ -RAY SYSTEM

E. IUCIUC, P. TRACZ^a, H. SCHUBERT

Extreme Light Infrastructure - Nuclear Physics, Horia Hulubei National Institute
of Physics and Nuclear Engineering, Măgurele-Bucharest, Romania
Corresponding author^a: piotr.tracz@eli-np.ro

Received September 8, 2023

Abstract. The paper presents results from computer simulations performed on a model of an RF electron source for the Laser Compton Scattering (LCS) γ -ray system. The new LCS γ -ray system is under implementation at ELI-NP/IFIN-HH. Different configurations of the system modelled with the ASTRA software package and different settings on the system components were analysed to optimize the initial beam parameters before acceleration up to ultra-relativistic energy in linac. The properly designed RF electron source contributes significantly towards delivery a high brightness beam, which is a crucial specification for the LCS γ -rays systems.

Key words: RF electron accelerator, LCS γ -ray system, computer simulations with ASTRA, modelling of electron beam, S-band RF system.

DOI: <https://doi.org/10.59277/RomJPhys.2023.68.304>

1. INTRODUCTION

The development of high energetic photon sources based on the Laser Compton Scattering is currently in progress [1–3]. The LCS γ -ray sources find applications in medicine, industry, nuclear waste treatment, and opened new opportunities for fundamental research in nuclear photonics, photo-fission, and astrophysics [4–7]. The “Compton Scattering” is a basic nuclear process in which an incident photon scatters off a low bound electron in an atom electronic shell. The initial photon transfers energy to the scattered electron. The photon energy is decreased, and the electron gains the extra energy. The inverse “Laser Compton Scattering” is an opposite mechanism and takes place when a high energy electron interacts with a photon. It results in high energy backscattered photon. Because the cross-section of the interaction is very low, a crucial specification for any γ -ray beam system based on the LCS are a high brightness electron beam and a photon beam with the high spectral density. The high brightness electron beams have already been used at Free Electron Lasers for more than 30 years [8–10]. The technological advance in the field of a high energy and high-performance lasers occurred in recent years, launching a huge effort to develop new generations of light sources for extremely high-quality x- and γ -rays. For a ‘back scatter’ geometry where the laser pulse and the electron bunch are counter

Romanian Journal of Physics **68**, 304 (2023)

propagating, the maximum energy of the scattered γ -ray photons E_γ is proportional to the square of the electron energy γ_e and to the incident photon energy E_L (in units of rest mass $\gamma_e = E_e/0.511$ MeV):

$$E_\gamma \simeq 4\gamma_e^2 \cdot E_L \quad (1)$$

The equation (1) drives design criteria for a choice of suitable laser wavelengths and electron energies to achieve the demanded E_γ . The fundamental design goal is to generate a high flux. Therefore, Luminosity L parameter is a good figure of merit applicable to LCS devices. It is defined as rate of scattering events N given an interaction cross-section σ , $L = \sigma^{-1} \cdot dN/dt$. The luminosity of two colliding Gaussian beams is expressed in terms of particle density, given by the number of particles in each beam N_1 electrons and N_2 photons, divided by quadrature addition of rms sizes at interaction point, σ_1 and σ_2 , and multiplied by the interaction rate or the frequency of collision rate f :

$$L = \frac{N_1 N_2}{2\pi(\sigma_1^2 + \sigma_2^2)} f \quad (2)$$

where $\sigma_1 = \sqrt{\beta\epsilon}$, and β is the Twiss parameter determining the shape and orientation of the electron bunch, ϵ is the beam emittance. To optimize the luminosity, it is necessary to enlarge the rate of interaction, or the number of particles in both beams, and compress the bunch. The electron beam is created and accelerated to relativistic energy in a radio frequency accelerator, designed for low emittance beam with high current, small energy spread, and short bunch, optimally collimated at the interaction region. If both electron and photon beams are focused to small spots and bear large energies, the LCS γ -ray sources produce large peak brightness.

The advanced Variable Energy Gamma (VEGA) System is under implementation at ELI-NP [11] as one of the major components of the infrastructure developed in Bucharest-Magurele, Romania. The extreme γ -ray beams will be dedicated for nuclear physics and nuclear photonics experiments, open for worldwide users. The VEGA system consists of an RF electron source, an RF linear accelerator (linac), a storage ring, and an advanced optical cavity where the interaction point is located. The VEGA system design specification is presented in Table 1.

The paper presents results received from running the computer simulations performed on the model of the RF electron source. The aim is to investigate different configurations of the system for optimization of the beam parameters before acceleration in the linac. The ultra-relativistic beam from the linac will be then injected to the storage ring. The system of the RF electron source is modelled with the ASTRA [12, 13], the software package for tracking particle beams under influence of external and internal fields. User defines the external fields, magnetic field of solenoids

Table 1

VEGA System Specification

Maximum photon energy	MeV	≥ 19.5
Tunability of Photon Energy		Yes
Linear Polarization of γ -Ray Beam ^{a)}	[%]	≥ 95
Divergence at FWHM of Beam Spot ^{a)}	[rad]	$\leq 1.5 \times 10^{-4}$
Average Relative Bandwidth of γ -ray Beam (FWHM) ^{a)b)}		$\leq 5.0 \times 10^{-3}$
Total Photon Flux ^{a)}	[1/s]	$\geq 1.1 \times 10^{11}$
Time-Average Spectral Density at Peak Energy		$\geq 5.0 \times 10^3$

^{a)} for all γ -ray energies;

^{b)} at reference-point located at approx. 10 m downstream of Compton collision point for γ -ray production.

and quadrupols, and electromagnetic fields of resonant/standing wave and accelerating/travelling wave cavities. The user defines also the input parameters for a generation of an initial particle distribution from a cathode. The software calculates the internal fields based on the magnetic elements and the particle beam definition. The internal fields result from the space charge effect which is dominant in non-relativistic beams. The ASTRA delivers different options for accurate calculation of the beam parameters resulted from the modelled system.

2. MODEL OF RF ELECTRON SOURCE

The model of the RF electron source consists of an RF gun cavity, a standing-wave (SW) cavity, and a set of solenoid magnets. The electrons are released from the cathode, and pre-accelerated in the RF gun cavity. The geometry of the gun cavity is based on the design of the BNL/SLAC/UCLA 1.6 cell RF gun, with accelerating π -mode, which is resonant at 2856 MHz (S-band) [14]. The extracted electrons leave the cathode in sort of a shower in any direction and repel one another by virtue of the space-charge effect what prevents the generation of the low emittance beam. Therefore the electrons must be captured and lumped into a defined bunch. That is initially done by solenoids, which are located near the gun cavity. The magnetic field from the solenoids counteracts the space-charge effect. The beam leaving the gun cavity has an energy of a few MeV. At this energy it is not yet stable against phase space oscillations in linear accelerators and particles make significant movement inside the bunch, leading to longitudinal instability. Therefore the SW cavity will work with a negative acceleration phase in order to confine the beam longitudinally while the solenoids are used to confine the beam radially.

Different configurations for the RF electron source system were investigated

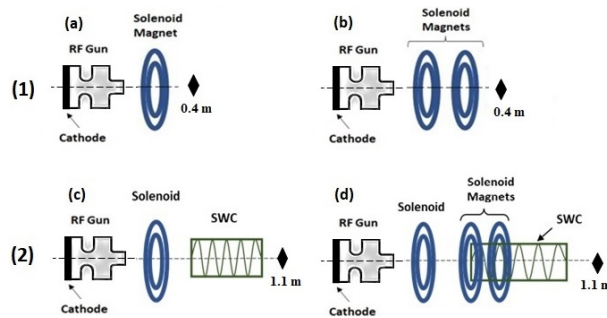


Fig. 1 – Different configurations of RF electron source. Positions for outputs generation are at distance 0.4 m and 1.1 m from cathode.

(Fig. 1). The first (1) considers the RF gun and solenoid magnets in two arrangements, *i.e.*, with a single solenoid, and with the Helmholtz Coil (HC). The second configuration (2) includes the SW cavity. The operating frequency of the cavities is 2.856 GHz. For the RF gun, the field gradient is 120 MV/m (max, at the cathode), and for the SW cavity is 28 MV/m. The field input phase at the RF gun was fixed at 0° , and for the SW cavity the input phase was varied (the simulations started with $\Phi = 0^\circ$) in order to find the best suited value for it.

3. INITIAL BEAM CONFIGURATION

The ASTRA program reads the initial particle coordinates from a file, which was generated by the ASTRA sub-program *Generator*. The 2D truncated Gaussian particle distribution in horizontal and vertical directions was implemented. The rms bunch size was set to $\sigma_x = \sigma_y = 1.2$ mm. There is another parameter specified, C_{Cut} , which determines intervals in horizontal $|x| \leq C_{Cut}\sigma_x$ and vertical $|y| \leq C_{Cut}\sigma_y$ directions. The C_{Cut} parameter cuts off the Gaussian distribution at $C_{Cut}\sigma$, and was introduced due to the limited aperture of the system. The particles were emitted from the plane cathode with a time spread. The plateau distribution was selected for the longitudinal particle distribution. The initial bunch length was set to 5 ps and the rise time rt to default value, 0.0 ns. For a good statistic approach, 40 000 particles were implemented in simulations. The total electron bunch charge was set to 1 nC. The Figure 2 presents the initial bunch dimension in transverse plane, and illustrates the particle distribution in the horizontal and vertical planes. The initial beam configuration, emitted from the cathode, is summarized in Table 2.

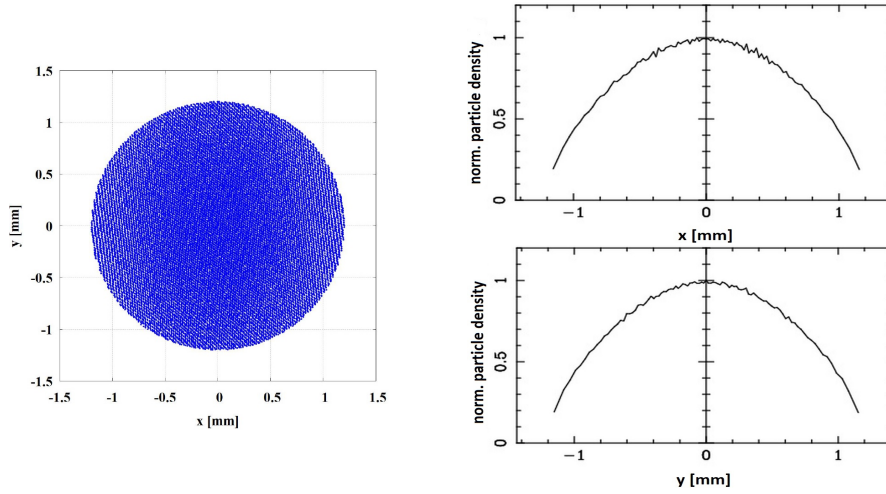


Fig. 2 – Initial particle distribution.

Table 2

Initial beam configuration

Number of particles	40 000
Total charge	1 nC
Trans. particle distribution	truncated Gaussian
RMS bunch size	1.2 mm
Long. particle distribution	plateau
RMS value of emission time	5 ps

4. RESULTS FROM COMPUTER SIMULATIONS

Series of computer simulations and analysis of results were performed to select the optimal configuration and appropriate settings for the RF electron source components. The Figure 3 compares the emittance and the beam spot size *versus* the position of the solenoids for different strengths of the magnetic field. For the single solenoid in use (configuration 1a, see Fig. 1), the emittance acquires lowest value at the distance (0.14 - 0.15) m from the cathode and the magnetic field 0.36 T. The higher field amplitudes result in over focusing of the beam and the emittance increases with the field strength. The beam spot decreases in size with increase of the solenoid distance and the magnetic field strength. The configuration 1b with the Helmholtz Coil (HC) indicates the lowest values of the emittance approximately at 0.154 m and 0.24 T. The over focusing effect, with the field strength increasing, is

not well manifested here. The beam spot size for a given position at a given field decreases with the field strength.

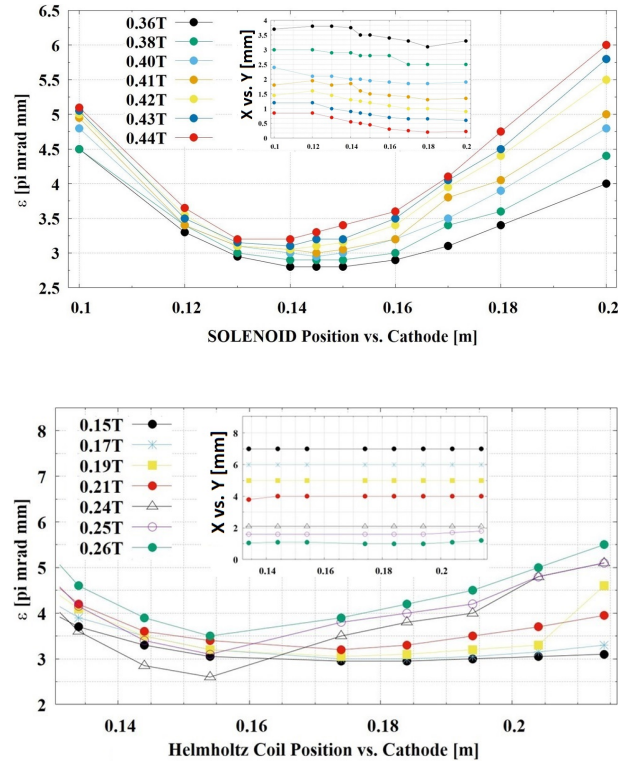


Fig. 3 – Transverse core emittance (95% particles) and beam spot size vs. position of solenoid magnets and magnetic field amplitude. ‘X’ and ‘Y’ are radius of full horizontal and vertical beam spot size.

Another investigated configurations include the SW cavity (2c and 2d, Fig. 1). Considering the results presented in Fig. 3, it was decided to locate the first solenoid at 0.14 m from the cathode, and the field amplitude set to 0.42 T. This selection is a compromise between the limit of the system aperture and the lowest possible emittance. The Figure 4 presents the emittance and the beam spot size *versus* the SW cavity position for the system with one solenoid (configuration 2c). The lowest value of the beam spot size is received at 0.4 m, and also the emittance is minimized at (0.2 - 0.4) m. It was observed significant increase of the spot size and the emittance *versus* the results presented in Fig. 3 (top). Nevertheless, Fig. 4 presents the results at 1.1 m *i.e.*, after the beam traversed the EM field of the SW cavity, and Fig. 3 the results at 0.4 m *i.e.*, straight after the solenoid. To maintain the regime of the low beam spot and emittance it was necessary to add other magnetic components in the system model. In the next step, the HC was implemented with the field amplitude set

to 0.24 T, and the location of the SW cavity was fixed at the distance 0.4 m from the cathode. The Figure 5 presents the emittance and the beam radial geometry for the system with three solenoids (configuration 2d, see Fig. 1). The HC location at 0.55 m was selected for running next simulations. This selection follows the results and is a bit arbitrary with the comment that the field strength is considered here as "non-fixed yet" and "to be optimized". Both the emittance and the beam spot in non-relativistic systems are heavily influenced by the magnetic field of solenoids. The position 0.55 m demonstrates the smallest emittance and therefore leads to the highest luminosity according to equation (2). Comparison of Figs. 4 and 5 makes it evident, the HC reduces the radial geometry of the beam by a factor of 4. It is significantly smaller at each analyzed HC position.

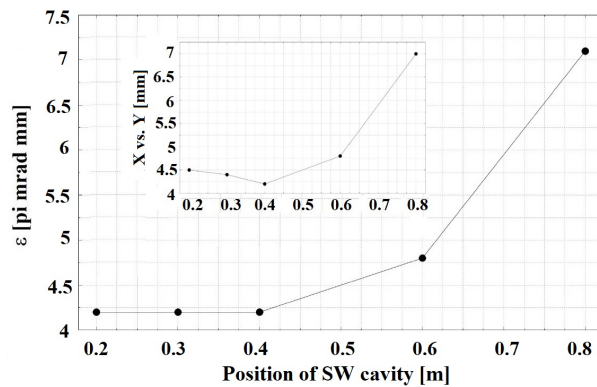


Fig. 4 – Transverse core emittance (95%) and beam spot size vs. position of SW cavity ($\Phi = 0^\circ$).

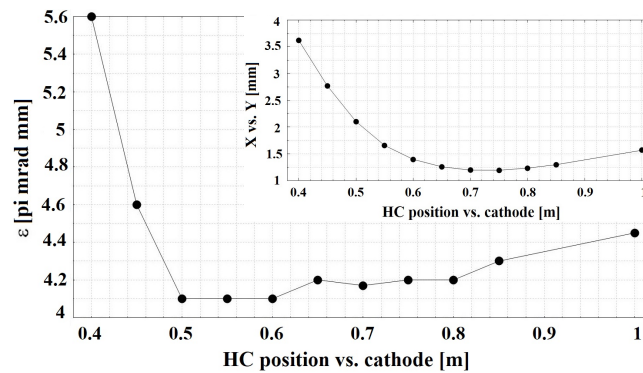


Fig. 5 – Transverse core emittance (95%) and beam spot size vs. HC position ($\Phi = 0^\circ$).

In the next step, the magnetic field strength of the HC was optimized. The Figure 6 depicts the emittance and the beam spot size in relation to the field amplitude.

The horizontal axis represents the field at each solenoid, the resultant field is stronger accordingly. The 0.5 T was considered as the optimal result, which keeps the regime on the low emittance and still accepted in respect to the spot size and aperture limit.

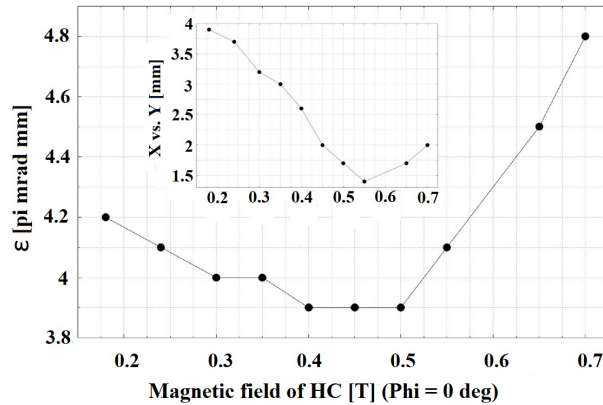


Fig. 6 – Transverse core emittance (95%) and beam spot size vs. HC magnetic field ($\Phi = 0^\circ$).

The simulations on the system with configurations 2c and 2d (results presented in Figs. 4, 5 and 6) were performed with the 0 deg input phase of SW cavity electric field. The electron beam is bunched thus the electric field input phase affects significantly the beam parameters. Other investigations were carried out to optimize this setting for the SW cavity. The energy spread (Fig. 7), the emittance and the beam spot (Fig. 8), and the beam divergence (Fig. 9) *versus* the E-field input phase are presented for system configuration 2d. The input phase was varied between -120 deg and 40 deg.

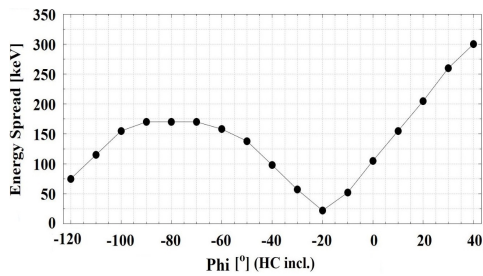


Fig. 7 – Energy spread (rms).

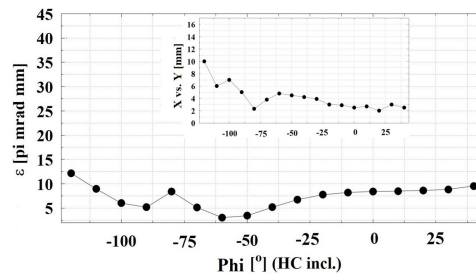


Fig. 8 – Emittance (95%) and beam spot.

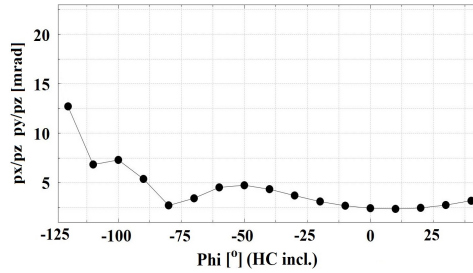


Fig. 9 – Beam Divergence (rms).

The bunch length *versus* the input phase is presented in Fig. 10 (left) and the beam energy in Fig. 10 (right). The bunch length is shortened up to 0.1 mm at -120° , then the lengthening occurs and it comes into saturation, reaching 0.62 mm at 40° . The bunch shortening by the phase variation takes place at the expense of the beam energy. The highest energy is received at the crest of the electric field *i.e.* at $\text{Phi} = 0^\circ$, with no bunch shortening or longitudinal focusing/confinement, which can lead to longitudinal instability further on in the accelerator system.

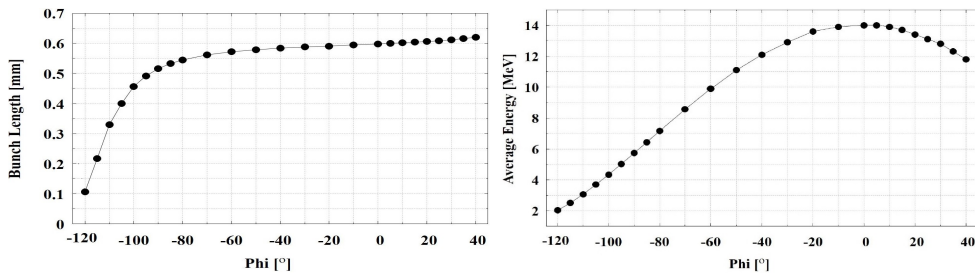


Fig. 10 – Bunch length (left) and Beam energy (right) vs. SW cavity input phase.

The optimal acceleration phase is a compromise between -20° (minimum energy spread, see Fig. 7), -60° (minimum emittance, Fig. 8) and 0° (maximum acceleration rate/beam energy, Fig. 10 right). It was considered the value of -30° as a good trade-off in setting for the input phase of the SW cavity E-field.

5. CONCLUSIONS

The results from the computer simulations performed on the model of the RF electron source for future LCS γ -ray system at ELI-NP were presented. The simulation model was investigated in different configurations with the electron gun cavity, the solenoid magnets, and the SW cavity. The RF electron source for the VEGA is the S-band system with the frequency operation of 2856 MHz. It acts major role for

shaping the electron beam and forming the beam parameters, which will be accelerated in linac and then injected to the storage ring. The beam is created and the bunch is initially shaped in the RF gun cavity. The solenoid magnets confine the beam near the axis, reducing the radial spread that occurs due to the space charge effect. The SW cavity affects the beam energy, bunch length and energy spread. The computer simulations were run with the different settings of the components' parameters, and the different arrangements of the components. The optimal location of the components and the system configuration are illustrated in Fig. 11. The Table 3 and 4 summarize the settings which, based on the results, were considered as the optimal choice. Also, the obtained beam parameters are presented.

The results and following analysis provided promising outcome for succeeding research for optimization of the linac design. It will be used as a guidance during the commissioning of the VEGA RF electron source as well as in research for the system development to meet requirements imposed by the future users.

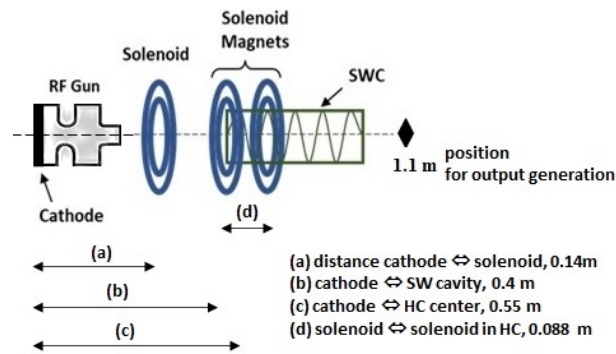


Fig. 11 – Optimal configuration of RF electron source.

Table 3

Components settings

Parameter	RF Gun	SW Cavity
E-field (max) [MV/m]	120	28
Input phase [°]	0.0	-30
Parameter	Solenoid	HC
M-field (max) [T]	0.42	0.5 (at each coil)

Table 4

Beam parameters from simulations

Parameter	Specification	Simulation
Energy gain [MeV]	>10	14 (max)
ϵ [π mrad mm]	<5	<4
En. spread rms [keV]	<100	25 (min)
Bunch length [mm]	<1	0.6 mm

Acknowledgements. This work was carried out under the contract PN 23.21.01.06 sponsored by the Romanian Ministry of Research, Innovation and Digitalization.

REFERENCES

1. Z. Hao, G. Fan, H. Wang *et al.*, Nucl. Instrum. Methods Phys. Res. A **1013**, 13-17 (2021).
2. C. R. Howell, M. W. Ahmed, A. Afanasev *et al.*, J. Phys. G: Nucl. Part. Phys. **49**, 010502 (2022).
3. D. Habs, M. Gunther, M. Jentschel *et al.*, AIP Conference Proceedings **1462**, 177-184 (2012).
4. H. Hina, M. Nafees, T. Ahman, Heliyon **7**, e05972 (2021).
5. J. Rico, Proc. of Sci., July (2011).
6. L. Senis, V. Rathore, A. Anastasiadis *et al.*, Nucl. Instrum. Methods Phys. Res. A **1014**, 165698 (2021).
7. D. Gao, X. Meng, H. Jin *et al.*, Magnetic Resonance Imaging **92**, 251-259 (2022).
8. C. Vaccarezza, D. Alesini, M. Anania *et al.*, Nucl. Instrum. Methods Phys. Res. A **829**, 237-242 (2016).
9. E. Eggl, M. Dierolf, K. Achterhold *et al.*, Journal of Synchrotron Radiation **23**, 1137-1142 (2016).
10. A. Bacci, D. Palmer, L. Serafini *et al.*, IPAC **2014**, 2238-2241 (2014).
11. Extreme Light Infrastructure - Nuclear Physics, <https://www.eli-np.ro/rd2.php>
12. K. Floettmann, Phys. Rev. Special Topics - Acc. and Beams **6**, 1-7 (2003).
13. K. Flottmann, ASTRA Manual **3.2**, 1-117 (2017).
14. Particle Beam Physics Lab., Photoinjector, http://pbpl.physics.ucla.edu/pages/pbpl_photoinjector.html